Microcirculation (2003) 10, 463–470

www.nature.com/mn

Blood–Brain Barrier Permeability Precedes Senile Plaque Formation in an Alzheimer Disease Model

MAKI UJIIE,*† DARA L. DICKSTEIN,*†‡ DOUGLAS A. CARLOW,† AND WILFRED A. JEFFERIES*†‡§

*Biotechnology Laboratory, University of British Columbia, Vancouver V6T 1Z3, Canada; †Biomedical Research Centre, University of British Columbia, Vancouver V6T 1Z3, Canada; ‡Department of Medical Genetics, University of British Columbia, Vancouver V6T 1Z3, Canada; §Department of Microbiology and Immunology, University of British Columbia, Vancouver V6T 1Z3, and Department of Zoology, University of British Columbia, Vancouver V6T 1Z4, Canada

ABSTRACT

Objective: To establish the generality of cerebrovascular pathology frequently observed with Alzheimer disease, we have assessed blood–brain barrier (BBB) integrity using the Alzheimer disease model Tg2576 mice in which cognitive deficits and neuritic plaque formation develop around 10–12 months of age.

Methods: We assessed BBB integrity using well-established methods involving albumin and Evans blue uptake and introduce the use of a novel perfusion protocol using succinimidyl ester of carboxyfluorescein diacetate.

Results: BBB permeability is increased in the cerebral cortex of 10-month-old Tg2576 mice preceding Alzheimer disease pathology presentation. Furthermore, when compared with their nontransgenic littermates, 4-month-old Tg2576 mice exhibit compromised BBB integrity in some areas of the cerebral cortex. An age-related increase in albumin uptake by the brains of Tg2576 mice, compared with nontransgenic mice, was also observed. These findings were supported by quantitative Evans blue analysis ($p = 0.07$, two-way analysis of variance).

Conclusion: A breakdown of BBB was evident in young 4- to 10-month-old Tg2576 mice. Compromised barrier function could explain the mechanisms of Aβ entry into the brain observed in experimental Alzheimer disease vaccination models. Such structural changes to the BBB caused by elevated Aβ could play a central role in Alzheimer disease development and might define an early point of intervention for designing effective therapy against the disease.
Microcirculation (2003) **10,** 463–470. doi:10.1038/sj.mn.7800212

KEY WORDS: Alzheimer disease, blood–brain barrier, beta-amyloid, transgenic mouse Tg2576, perfusion, succinimidyl ester of carboxyfluorescein diacetate

INTRODUCTION

Alzheimer disease (AD) is the most common form of dementia and a growing public health concern for the aging world population. The connection between cerebrovascular conditions and AD has been overlooked until recently, because occurrence of stroke before exhibition of AD-like symptoms excludes patients from being diagnosed with AD. Despite this, amyloid angiopathy is frequently associated with AD and is being increasingly accepted as another distinguishing feature of the disease in addition to AD hallmarks of senile plaques and neurofibrillary tangles. In fact, approximately 90% of AD brains are reported to have cerebrovascular amyloid consisting mostly of amyloid beta (Aβ) in small arteries, arterioles, and capillaries (26). Cerebral amyloid angi-

Funded by the Canadian Institute for Health Research (grant numbers MT-14408 and MOP-49531).
For reprints of this article, contact Wilfred A. Jefferies, The Biotechnology Laboratory and the Biomedical Research Centre, University of British Columbia, 2222 Health Sciences Mall, Vancouver, B. C. Canada V6T 1Z3; e-mail: wilf@brc.ubc.ca.
Received 9 April 2002; accepted 10 February 2003

opathy (CAA) is also frequently present in the elderly without AD and is exhibited in 50% of the population at the age of 90 (26). Determining whether and when cerebral microvessels become compromised in AD is of considerable importance, because it could define an early therapeutic intervention point to slow down the progression of the disease. In addition, the increase in BBB permeability might explain why peripheral pools of Aβ gains access to the brain to protect it from further damage in the case of Aβ vaccination (10,15).

The brain has a unique structural barrier termed the blood–brain barrier (BBB), which functions to restrict most large and/or hydrophilic molecules from entering the parenchyma. In pathology, the BBB often becomes compromised, and the brain becomes vulnerable to exposure to various factors in the blood. Conventional histochemical methods for studying BBB integrity are based on the exclusion of defined molecules that do not access the brain under normal conditions. For example, albumin is a 70-kDa endogenous serum protein widely used to study BBB breakdown, because its transporter, gp60, is nearly absent in brain endothelia (23). Another commonly used tracer, horseradish peroxidase, is a 40-kDa plant glycoprotein. It does not bind to plasma membrane or cross the BBB with high efficiency, because it is transported by way of pinocytotic vesicles that are rarely observed in cerebral endothelial cells. These two proteins have been shown not to alter BBB integrity at the dosages used in routine experiments. As well, various dyes such as Evans blue, trypan blue, and fluorescein, in addition to several radiotracers, have been injected into animals to study structural changes of the BBB.

With the purpose of complementing conventional histochemical procedures used in BBB research, we designed a new application for a widely used compound, the succinimidyl ester of carboxyfluorescein diacetate (5[6]-CFDA SE), involving whole-body perfusion and consequent labeling of endothelial cells to study the relationship between increased levels of Aβ and BBB permeability in an AD model mouse. There are three major advantages associated with the use of CFDA SE for such studies. First, once CFDA SE enters endothelial cells, it will undergo cleavage by intracellular esterase, thereby becoming irreversibly coupled to intracellular proteins. Thus, the fluorescent product, CFSE, does not travel farther into tissues in the presence of a barrier and will not be transferred into neighboring cells. Second, CFDA SE is well tolerated by many cell types and is unlikely to alter BBB morphology. This is demonstrated by the fact that CFDA SE is the preferred choice for researchers to track migratory cells during multiple cell doublings. Third, perfusion with CFDA SE is a rapid labeling method that results in a relatively bright and stable fluorescent product that can be studied with various types of fluorescence microscopes.

To date, several models of mice have been generated that partially mimic the neurologic signs and pathology of AD. These transgenic mice make it possible for investigators to focus and to analyze the effect of a small number of key factors involved in the progression of AD. One of these models, Tg2576 overexpressing human amyloid precursor protein (APP), contains the Aβ double Swedish mutations K697N and M671L at the site of β-secretase cleavage. The resulting increase in $A\beta_{1-42}$ and $A\beta_{1-40}$ production leads to substantial diffuse and neuritic plaque formation around 10–12 months of age (8,9,11,19). Vascular amyloid deposits in the brain are also observed around 20 months of age in these mice (13). In addition, Tg2576 mice develop age-dependent behavioral deficits as assessed by the Y maze and Morris water maze tests around 10 months of age (2,8). Because the cellular, anatomical, and behavioral changes are shared in human AD, we chose the Tg2576 AD model mice to study the effects of Aβ on the BBB in Tg2576 mice before major Aβ accumulation in the brain.

MATERIALS AND METHODS

Mice

An AD model transgenic mouse, Tg2576, was generated and generously provided by Hsiao et al. (7). It contains the human APP_{695} gene, with the Swedish double mutation K697N, M671L, under the control of the hamster prion protein promoter (8), resulting in overexpression of human amyloid precursor protein by the brain (21). The mice were kept and bred at an animal care unit at the University of British Columbia. The Tg2576 mice were genotyped at 2 weeks of age as previously described (8), and 4- to 18-month-old mice were used for this experiment. Non-Tg littermates were used as controls whenever possible, otherwise age-matched non-Tg mice were used as controls. Transgenic mice were purchased from Charles River Laboratories (Wilmington, MA), and C57Bl/6 mice were purchased from Jackson Laboratories (Bar Harbor, ME). All experiments were conducted in compliance with the Canadian Association for Accreditation of Laboratory Animal Care.

Perfusion and Tissue Processing

For morphologic analysis of the BBB, the mice were anesthetized with ketamine (25 mg/kg i.p.) and xylazine (5 mg/kg i.p.), transcardially perfused with 10 μM, 20 μM, or 50 μM CFDA SE (Molecular Probes, Eugene, OR) in Media 199 (Invitrogen, Burlington, ON, Canada) for 3 minutes, which was followed by 4% formaldehyde in PBS. Some mice were injected in the tail vein with 100 μg of Texas red conjugated bovine serum albumin (Molecular Probes) 1 hour before CFDA SE perfusion. Alternatively, one 10-month-old Tg2576 mouse was perfused without CFDA SE to investigate autofluorescence. In all mice, the organs were immediately dissected out and postfixed for 24 hours in 4% formaldehyde. For fluorescence dissecting microscopic observation of C57bl/6 mice, approximately 5-mm slices of brain and liver were manually cut with a razor blade and viewed under the microscope. Thymus, kidney, and testes were manually cut in halves and also viewed under the fluorescence dissecting microscope. Other samples were processed for paraffin embedding and coronally sectioned at approximately 6 μm. The sections were mounted onto slides and viewed using BioRad Radiance fluorescent confocal microscope (BioRad Cell Science, Hercules, CA).

The age-depended accumulation of senile plaques in the Tg2576 brain was visualized with Congo red. Mice were anesthetized and transcardially perfused with PBS followed by 4% formaldehyde as described previously. The brains were paraffin embedded, sectioned, stained for Congo red, and counterstained with hematoxylin using standard procedure.

Evans Blue Analysis

Quantitative Evans blue analysis was carried out as previously described (14,25) with some modifications. Tg2576 mice and their age-matched controls were weighed and intraperitoneally injected with 50 μg/g Evans blue dye (n = 13). Three hours after injection, the mice were anesthetized with ketamine (25 mg/kg i.p.) and xylazine (5 mg/kg i.p.) and perfused with PBS for 5 minutes. After removing the cerebellum and olfactory bulbs, the brains were weighed; 1 mL of 50% trichloroacetic acid was added, and the brains were dounce homogenized. The samples were centrifuged at 13,000 rpm for 10 minutes, and the supernatant was diluted 1:4 with 100% ETOH. Evans blue fluorescence was read with an ELISA plate reader (Spectra Max 190; Molecular Devices, Sunnyvale, CA) at 620 nm. The readings were divided by the weight of the brain, and the data were statistically analyzed with two-way analysis of variance.

Acquisition of Image

A Leica MZFLIII stereo fluorescence dissecting microscope (Leica Microsystems, Richmond Hill, ON, Canada) and BioRad Radiance fluorescence confocal microscope were used to capture the images. For both microscopes, the argon ion laser was emitted at 488 nm to excite CFDA SE. Doubly fluorescent sections were visualized by adding a helium neon laser emitted at 570 nm to excite Texas red–conjugated BSA. The single color confocal images were sequentially collected and superimposed to make two color images. For all experiments, controls and CFDA SE–perfused sections were analyzed under identical settings (scanning dimension, laser power, gain, and aperture size) for all experimental and control groups. An exception was made to detect autofluorescence in a 10-month-old Tg2576 mouse in which the laser power, gain, and aperture size were approximately doubled, because the settings for CFSE detection were insufficient to visualize autofluorescence. All images were processed using NIH Image 1.92 and Adobe Photoshop 5.5.

RESULTS

To determine the optimal perfusion concentration of CFDA SE to study the BBB, C57Bl/6 mice were perfused with 10, 20, and 50 μM CFDA SE. The confocal images show that the cerebral microvessels (Fig. 1), in addition to larger vessels (Fig. 2a) were fluorescently labeled with CFSE at 10 μM. Furthermore, no apparent difference in labeling intensity or distribution was observed when mice were perfused with 10 μM, 20 μM, or 50 μM CFDA SE (Fig. 1). This might be due to intraendothelial esterases becoming saturated at 10 μM, and we concluded that

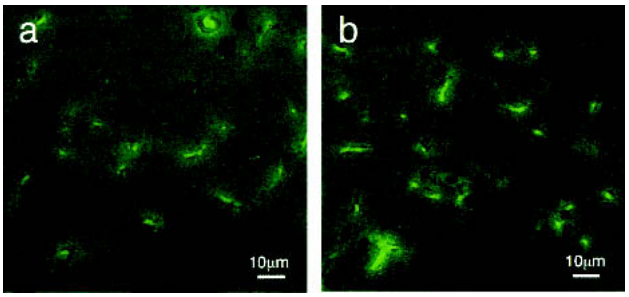

Figure 1. C57Bl/6 mice perfused with various concentrations of CFDA SE. In the cerebral cortices of mice perfused with 10 μM (a) or 50 μM (b) CFDA SE, only the endothelia exhibited fluorescence at either concentration.

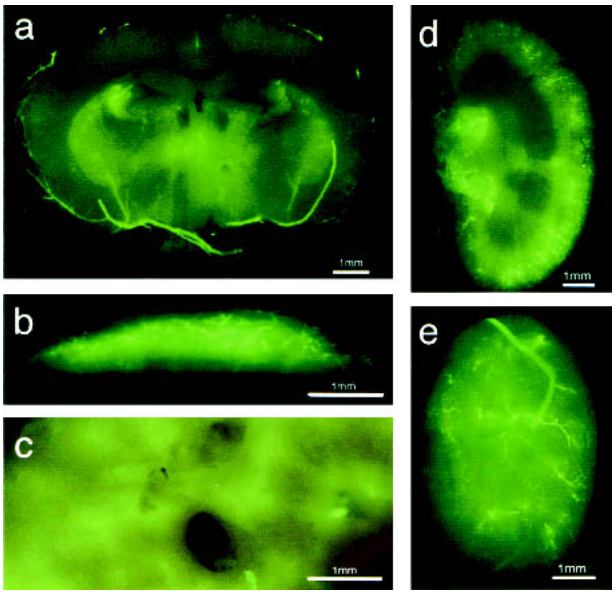

Figure 2. Various organs of C57Bl/6 mice perfused with CFDA SE. Brain (a), thymus (b), liver (c), kidney (d), and testes (e) were observed under a fluorescent dissecting microscope. Green fluorescence seems to be contained in blood vessels of organs with barriers (brain, thymic cortex, kidney, and testes), whereas barrier-free organs exhibit diffuse fluorescence (thymic medulla and liver).

10 μM CFDA SE was adequate to visualize cerebral microvessels. Because 10 μM is within the range of concentrations for long-term labeling of cells recommended by the manufacturer, the dosage seemed to be well tolerated by endothelial cells, and no morphologic alteration caused by CFDA SE perfusion was evident in the cerebral microvasculature.

The labeling pattern after CFDA SE perfusion was then examined in various organs from C57Bl/6 mice. Fluorescence in thick slices of the brain, kidney, thymus, testis, and liver were compared under low magnification with a fluorescence-dissecting microscope. We anticipated that the presence or absence of a barrier would be reflected in a differential staining pattern (Fig. 2). In the brain, a pattern of restricted fluorescence was seen in regions with BBB, whereas fluorescence was more diffuse around circumventricular organs, where communication between cerebrospinal fluid and the brain takes place. The pattern of restricted fluorescence was also observed for thymic cortex, kidney, and testes, which also have barrier structures (Fig. 2b, d and e, respectively). In tissues that do not have barriers, such as the thymic medulla and liver, CFDA SE penetrated throughout the tissue, labeling the parenchyma and endothelial cells (Fig. 2b and c, respectively). The dissecting micrograph of the brain combined with the confocal image (Fig. 1) show that CFDA SE effectively perfused through vessels of various diameters and was efficiently incorporated into endothelial cells.

In preparation for applying the new technique to analyze BBB permeability in Tg2576 mice, age-dependent accumulation of senile plaques in the cerebral cortices of Tg2576 was examined. As reported by other investigators, a few Congo-red–positive plaques began to be seen in the cerebral cortex of the Tg2576 mouse around 9 months of age (Fig. 3b). At 14 months, large and brightly labeled structures were abundant in the cerebral cortex (Fig. 3d). No staining pattern characteristic to neuritic plaques was seen in the cerebral cortices of either 9- or 14-month-old non-Tg mice (Fig. 3a and c, respectively). On the basis of these observations and a report that the BBB is breached in the human brain with high plaque burdens (26), we initially chose to study 10-month-old mice just as senile plaques are beginning to build up in the brain. Increased permeability of the BBB as indicated by extravascular

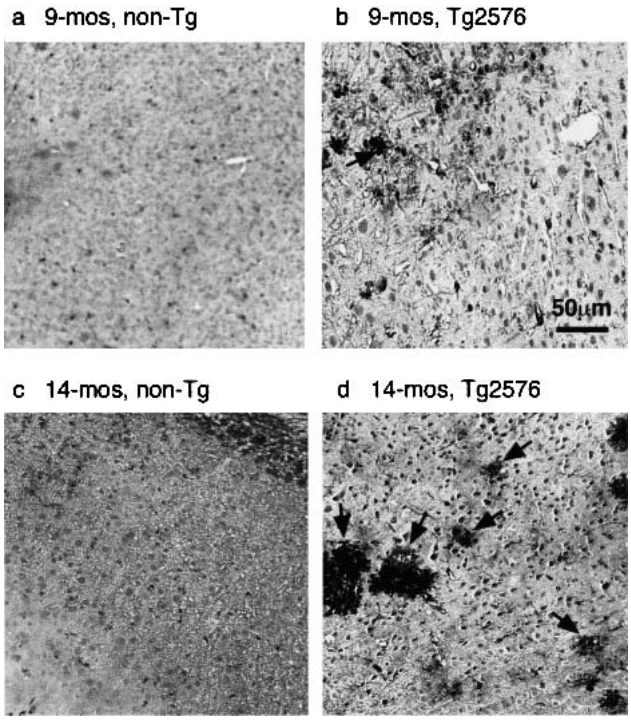

Figure 3. Age-dependent accumulation of senile plaques in Tg2576 cerebral cortex. Senile plaques (arrows) stained with Congo red begin to be seen in the 9-month-old Tg2576 cerebral cortex (b). The plaques (arrows) are more abundant in the 14-month-old Tg2576 cerebral cortex (d). Nontransgenic mice do not exhibit plaques in the brain regardless of age (a and c).

CFSE staining was noted in the cerebral cortex of 10-month-old Tg2576 brain compared with age matched non-Tg brain (Fig. 4a and b). The distinctive staining pattern in Tg2576 cerebral cortex was consistently observed. However, the location of fluorescence in the cerebral cortex differed somewhat from mouse to mouse. To rule out the possibility that the detectable green fluorescence was due to autofluorescence emitted by endogenous lipofuscin (excited at 458nm), CFDA SE perfused Tg2576 brain was compared with an age-matched Tg2576 mouse perfused with Media 199 alone (Fig. 4a and c). In the mouse perfused with media, some autofluorescence was detectable throughout the brain but only when laser power, iris size, and gain were doubled.

Because the use of the CFDA SE perfusion technique to examine BBB breakdown has not been previously tested, the brains of 10-month-old Tg2576 mice were further investigated using an existing method. BBB integrity is often examined by injecting labeled albumin and following its uptake by the brain, since albumin does not readily pass through an intact BBB. Thus, loss of BBB structure in Tg2576 could be visualized with both fluorescently labeled albumin and CFDA SE using a confocal microscope. We found that Texas red–conjugated BSA seemed to be excluded from entering the cerebral cortex in 10-month-old non-Tg mice (Fig. 4e), whereas it was prevalent in the Tg2576 cortex (Fig. 4h). CFDA SE perfusion resulted in brightly labeled vessels, but its extravascular cerebral cortical distribution did not always correspond to that of Texas red-BSA. This might be due to the reduced availability of intracellular esterases that are required to convert CFDA SE into fluorescent compounds, whereas uptake of Texas red-BSA is directly visualized.

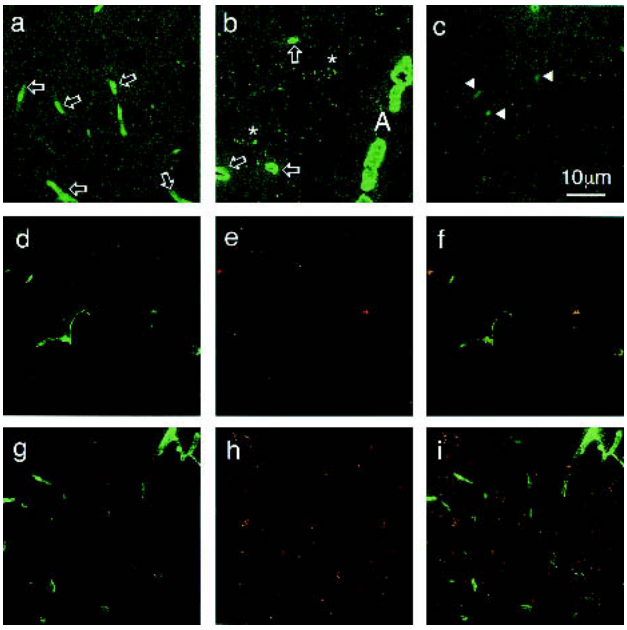

Figure 4. Blood–brain barrier permeability in 10-month-old Tg2576. Ten-month-old Tg2576 mice were perfused with CFDA SE (with the exception of d) to examine BBB permeability. Nontransgenic mouse cerebral cortex (a) shows little fluorescence beyond endothelia compared with Tg2576 mice (b). An arteriole in panel b is represented by A. Autofluorescence (solid triangles) was studied in a 10-month-old Tg2576 mouse that was not perfused with CFDA SE (c). Ten-month-old Tg2576 and non-Tg brains were further analyzed for their ability to take up Texas red–conjugated bovine serum albumin. Panels d and g show CFDA SE perfusion, (e) and (h) correspond to BSA, and (f) and (i) represent composites of red and green fluorescence in nontransgenic and transgenic mice, respectively. Open arrows indicate microvessels, and asterisks show fluorescence in the parenchyma.

In our effort to determine when BBB permeability occurs relative to the onset of AD signs, we examined the brains of younger Tg2576 mice. The results show that even at 4 months of age Tg2576 mice exhibit increased BBB permeability in some parts of the cerebral cortex compared with their non-Tg littermate control (Fig. 5a and b). The extent of extravascular CFSE distribution in the cerebral cortex was less evident in 4-month-old Tg2576 mice than in 10-month-old mice. As in the 10-month-old Tg 2576 mice, when 4-month-old mice were first injected with Texas red–conjugated BSA 1 hour before CFDA SE perfusion, red fluorescence was only seen in the cerebral cortex of the Tg2576 mouse (Fig. 5g) but not in the brain of its non-Tg littermate (Fig. 5d).

To test whether an increase in BBB permeability observed in many parts of the Tg2576 brain is a global phenomenon, Evans blue dye was injected into Tg2576 and non-Tg mice of various representative age groups; 4- and 8-month-old mice (reportedly lacking signs of AD), and 12- to 18-month-old mice (expected to have considerable neuritic plaque burdens in the brain). Increased uptake of Evans blue by the brains of Tg2576 mice compared with non-Tg mice was observed in every age group (Fig. 6). When these data were combined, Tg2576 brains exhibited increased BBB permeability compared with non-Tg mice (two-way analysis of variance with age and transgenic as two factors; $p = 0.066$).

DISCUSSION

We have designed a novel method for assessing BBB integrity using 5(6)-CFDA SE. Unlike other dyes or

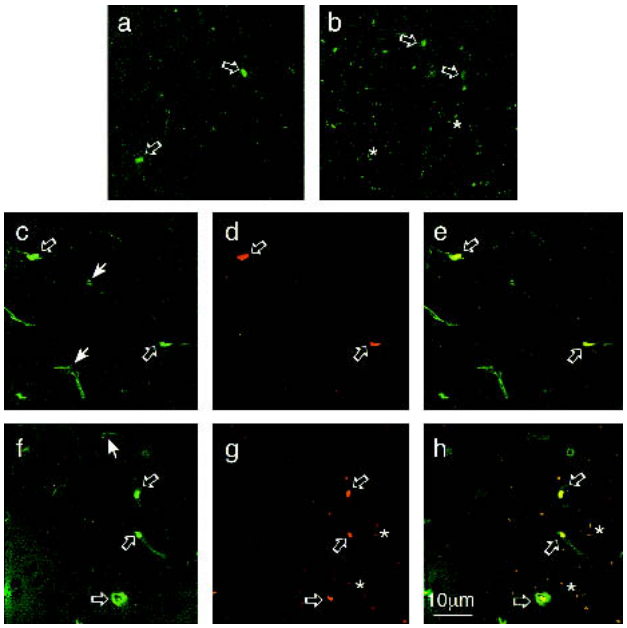

Figure 5. Blood–brain barrier permeability in 4-month-old Tg2576. The 4-month-old cerebral cortex in nontransgenic (a) and transgenic (b) cerebral cortices perfused with CFDA SE show that fluorescence is present in the parenchyma of the transgenic brain but not in control. Texas red–conjugated BSA was injected into the 4-month-old non-transgenic (c and e) and Tg2576 (f–h) mice 1 hour before CFDA SE perfusion. Panels c and f show CFDA SE perfusion, (d) and (g) correspond to BSA, and (e) and (h) represent composites of red and green fluorescence in nontransgenic and transgenic mice, respectively. Distribution of red fluorescence corresponding to BSA is limited to microvessels in nontransgenic cerebral cortex (d and e) but extends into parenchyma in the Tg2576 cortex (g and h). Open arrows indicate microvessels, and asterisks show fluorescence in the parenchyma. Solid arrows in (c) and (f) represent vessels without adhered or endocytosed BSA.

large molecules used to study cerebral microvessels, this molecule has a unique ability to enter cells and be intracellularly retained without being transferred into neighboring cells. In addition, information regarding the general health of a cell or tissue could be obtained using this method, because CFDA SE's conversion into a fluorescent compound is dependent on functional intracellular esterase. In this report, we show that when a mouse is perfused with CFDA SE, confined fluorescence is exhibited in barrier systems, including the brain, testes, thymic cortex, and kidney, whereas the barrier-free regions of thymic medulla and liver show diffuse fluorescence (Figs. 1 and 2). Using this technique to study the AD model Tg2576 mice, we found that BBB permeability in the cerebral cortex is already increased in 4-month-old Tg mice compared with their non-Tg littermates (Figs. 4 and 5). Furthermore, uptake of Texas red–conjugated BSA by the Tg2576 brain 1 hour after injection was notably higher than the control (Figs. 4 and 5). Increased disruption of the BBB seemed to correlate with age, and 10-month-old Tg2576 mice had fluorescence covering wider areas of cerebral cortex compared with 4-month-old mice (Figs. 3 and 4). Quantitative Evans blue analysis supported the finding that BBB is altered in Tg2576 mice compared with non-Tg mice before and after senile plaque buildup (two-way analysis of variance; $p = 0.07$). Collectively, these results strongly suggest that the BBB is severely damaged in the cerebral cortex by excessive exposure to Aβ even in the absence of well-defined senile plaques.

The finding that Aβ is either directly or indirectly responsible for endothelial toxicity is consistent with various studies. Treating cerebral endothelial cells with Aβ has been shown to increase transmigration of monocytes across a BBB model in vitro (5,6). When excised rat aorta was treated with Aβ, endothelial cells produced superoxide radicals (24), and a free radical formation inhibitor, N-tert-butyl-α(2 sulfophenyl)nitrone, protected primary brain endothelial cell cultures against Aβ toxicity (3). In addition to confirming the cytotoxic effect of Aβ on cerebral endothelial cells, our report shows that the role of BBB as the "gatekeeper" of the brain becomes compromised in the cerebral cortex in Tg2576 mice. In contrast, Poduslo et al., have shown that whereas the BBB structure is damaged by adherence of albu-

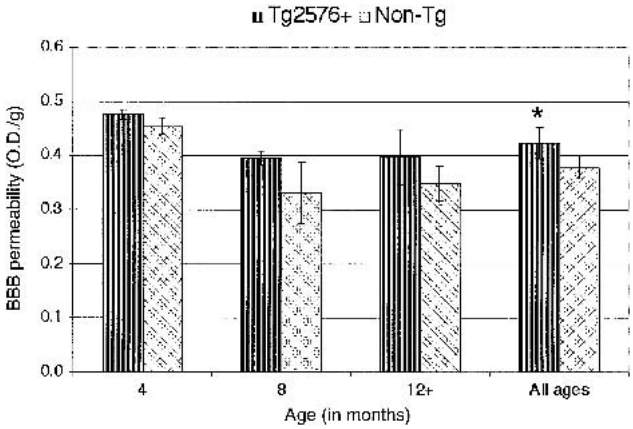

Figure 6. Analysis of BBB permeability using Evans blue dye. The uptake of Evans blue dye is graphed for transgenic2576 and non-Tg mice of various ages. Overall, Tg2576 exhibited increased BBB permeability compared with non-Tg (two-way analysis of variance; age and transgenic versus nontransgenic; $p = 0.07$*).

min to the BBB, permeability of the BBB to albumin is decreased in the adult AD model double transgenic mice (Tg2576/Presinilin-1) (18). The conflicting interpretations drawn in Poduslo's study and ours might be due to different experimental procedures or the transgenic model used. In addition, the authors mentioned that their physiologic study was more global and might not have accounted for local differences in the brain.

More important than establishing Aβ toxicity on endothelial cells, however, is the discovery that BBB disruption is manifested in 4-month-old Tg2576 mice, possibly leading the way for senile plaque formation and disease progression. No signs of AD are evident at this stage; however, significant levels of human APP are expressed in mice as early as 2 months of age in Tg2576 mice (11). AD is highly complex, and although it might be too early to speculate on the relationship between BBB disruption and etiology, alteration of BBB followed by a change in parenchymal environment is likely to be a key contributing factor in AD progression. We are currently conducting a more detailed study of BBB structure and function in various ages of Tg2576 mice that will allow us to better understand this relationship. We plan to eventually address BBB permeability in cerebral amyloid angiopathy, AD, and in patients with other forms of dementia.

The Aβ that exhibits toxicity on endothelial cells could come from three sources: brain, vasculature, or blood. Our observations strongly support the first view, that Aβ expressed in the brain is largely responsible for initiating BBB damage because although some Aβ is found in most organs of the Tg2576 mice, the brain accounts for nearly all human APP expression (11). However, our findings do not preclude the possibility that serum-derived Aβ contributes to BBB disruption to some degree, because higher plasma levels of both $A\beta_{42}$ and $A\beta_{40}$ are present in Tg2576 mice compared with non-Tg controls (11,13). A single injection of supraphysiologic concentration of insoluble $A\beta_{25\text{-}35}$ failed to induce changes in BBB permeability as assessed by CFDA SE perfusion in our study (data not shown); it is possible, however, that the cumulative effect of chronic exposure to serum Aβ could play a role in BBB disruption.

Noteworthy advances in AD research include the use of peripherally administered Aβ peptides as a possible AD vaccine in an effort to reduce senile plaque loads in the brain. Two studies reported reduced plaque burden in the brain and improved cognition in AD model mice after several months of treatment (10,15). When the protocol was tested in AD patients, however, increased inflammation and accelerated cognitive decline was exhibited in some cases, and the clinical trial was abandoned. It was later found that passive Aβ immunization in mice leads to cerebral microhemorrhage (17). The notion that a breach in the BBB is intimately associated with insoluble Aβ and thus AD suggests that peripherally administered Aβ gains access to the brain by way of a compromised BBB. Such BBB breakdown would also explain why the immune system is able to respond to Aβ or anti-Aβ antibody either to reduce the plaque burden in the immune-privileged brain after peripheral vaccination or to accelerate AD symptoms (10,15,20). The leaky BBB could also help explain the mechanism behind elevated levels of some proteins in the serum of AD patients, including p97 (12) and heme oxygenase-1 (22). A more complete picture of AD, integrating the relationship between Aβ and the BBB, is just beginning to emerge. Vascular accumulation of $A\beta_{42}$ and $A\beta_{40}$ in AD and other diseases is a well-documented risk factor for cerebral hemorrhage and atherosclerosis (1,4,16,26), calling for more research awareness. To this end, we are currently working to restore the integrity of the BBB in an attempt to slow down AD-like signs in Tg2576 mice.

ACKNOWLEDGMENTS

We thank Dr. Ian Clark-Lewis' Laboratory for synthesizing $A\beta_{25\text{–}35}$ and $A\beta_{35\text{–}25}$ peptides and Yulia D'yachkova for statistically analyzing the data. We also thank Drs. Brandie L. Walker and Cheryl G. Pfeifer for suggestions on the manuscript.

REFERENCES

1. Cadavid D, Mena H, Koeller K, Frommelt RA. (2000). Cerebral beta amyloid angiopathy is a risk factor for cerebral ischemic infarction. A case control study in human brain biopsies. *J Neuropathol Exp Neurol* 59:768–773.
2. Chapman PF, White GL, Jones MW, Cooper-Blacketer D, Marshall VJ, Irizarry M, Younkin L, Good MA, Bliss TV, Hyman BT, Younkin SG, Hsiao KK. (1999). Impaired synaptic plasticity and learning in aged amyloid precursor protein transgenic mice. *Nat Neurosci* 2:271–276.
3. Eisenhauer PB, Johnson RJ, Wells JM, Davies TA, Fine RE. (2000). Toxicity of various amyloid beta peptide species in cultured human blood-brain barrier endothelial cells: increased toxicity of dutch-type mutant. *J Neurosci Res* 60:804–810.
4. Ferreiro JA, Ansbacher LE, Vinters HV. (1989). Stroke related to cerebral amyloid angiopathy: the

significance of systemic vascular disease. *J Neurol* 236:267–272.

5. Fiala M, Zhang L, Gan X, Sherry B, Taub D, Graves MC, Hama S, Way D, Weinand M, Witte M, Lorton D, Kuo YM, Roher AE. (1998). Amyloid-beta induces chemokine secretion and monocyte migration across a human blood–brain barrier model. *Mol Med* 4:480–489.
6. Giri R, Shen Y, Stins M, Du Yan S, Schmidt AM, Stern D, Kim KS, Zlokovic B, Kalra VK. (2000). Beta-amyloid-induced migration of monocytes across human brain endothelial cells involves RAGE and PECAM-1. *Am J Physiol Cell Physiol* 279:C1772–C1781.
7. Hsiao K, Chapman P, Nilsen S, Eckman C, Harigaya Y, Younkin S, Yang F, Cole G. (1996). Correlative memory deficits, Abeta elevation, and amyloid plaques in transgenic mice. *Science* 274:99–102.
8. Hsiao KK, Borchelt DR, Olson K, Johannsdottir R, Kitt C, Yunis W, Xu S, Eckman C, Younkin S, Price D, Iadecola C, Clark HB, Carlson G. (1995). Age-related CNS disorder and early death in transgenic FVB/N mice overexpressing Alzheimer amyloid precursor proteins. *Neuron* 15:1203–1218.
9. Irizarry MC, McNamara M, Fedorchak K, Hsiao K, Hyman BT. (1997). APPSw transgenic mice develop age-related A beta deposits and neuropil abnormalities, but no neuronal loss in CA1. *J Neuropathol Exp Neurol* 56:965–973.
10. Janus C, Pearson J, McLaurin J, Mathews PM, Jiang Y, Schmidt SD, Chishti MA, Horne P, Heslin D, French J, Mount HT, Nixon RA, Mercken M, Bergeron C, Fraser PE, St George-Hyslop P, Westaway D. (2000). A beta peptide immunization reduces behavioural impairment and plaques in a model of Alzheimer's disease. *Nature* 408:979–982.
11. Kawarabayashi T, Younkin LH, Saido TC, Shoji M, Ashe KH, Younkin SG. (2001). Age-dependent changes in brain, CSF, and plasma amyloid (beta) protein in the Tg2576 transgenic mouse model of Alzheimer's disease. *J Neurosci* 21:372–381.
12. Kennard ML, Feldman H, Yamada T, Jefferies WA. (1996). Serum levels of the iron binding protein p97 are elevated in Alzheimer's disease. *Nat Med* 2:1230–1235.
13. Kuo YM, Crawford F, Mullan M, Kokjohn TA, Emmerling MR, Weller RO, Roher AE. (2000). Elevated A beta and apolipoprotein E in A betaPP transgenic mice and its relationship to amyloid accumulation in Alzheimer's disease. *Mol Med* 6:430–439.
14. Methia N, Andre P, Hafezi-Moghadam A, Economopoulos M, Thomas KL, Wagner DD. (2001). ApoE deficiency compromises the blood brain barrier especially after injury. *Mol Med* 7:810–815.
15. Morgan D, Diamond DM, Gottschall PE, Ugen KE, Dickey C, Hardy J, Duff K, Jantzen P, DiCarlo G, Wilcock D, Connor K, Hatcher J, Hope C, Gordon M, Arendash GW. (2000). A beta peptide vaccination prevents memory loss in an animal model of Alzheimer's disease. *Nature* 408:982–985.
16. Olichney JM, Hansen LA, Hofstetter CR, Grundman M, Katzman R, Thal LJ. (1995). Cerebral infarction in Alzheimer's disease is associated with severe amyloid angiopathy and hypertension. *Arch Neurol* 52: 702–708.
17. Pfeifer M, Boncristiano S, Bondolfi L, Stalder A, Deller T, Staufenbiel M, Mathews PM, Jucker M. (2002). Cerebral hemorrhage after passive anti-Abeta immunotherapy. *Science* 298:1379.
18. Poduslo JF, Curran GL, Wengenack TM, Malester B, Duff K. (2001). Permeability of proteins at the blood-brain barrier in the normal adult mouse and double transgenic mouse model of Alzheimer's disease. *Neurobiol Dis* 8:555–567.
19. Pratico D, Uryu K, Leight S, Trojanoswki JQ, Lee VM. (2001). Increased lipid peroxidation precedes amyloid plaque formation in an animal model of Alzheimer amyloidosis. *J Neurosci* 21:4183–4187.
20. Schenk D, Barbour R, Dunn W, Gordon G, Grajeda H, Guido T, Hu K, Huang J, Johnson-Wood K, Khan K, Kholodenko D, Lee M, Liao Z, Lieberburg I, Motter R, Mutter L, Soriano F, Shopp G, Vasquez N, Vandevert C, Walker S, Wogulis M, Yednock T, Games D, Seubert P. (1999). Immunization with amyloid-beta attenuates Alzheimer-disease-like pathology in the PDAPP mouse. *Nature* 400:173–177.
21. Scheuner D, Eckman C, Jensen M, Song X, Citron M, Suzuki N, Bird TD, Hardy J, Hutton M, Kukull W, Larson E, Levy-Lahad E, Viitanen M, Peskind E, Poorkaj P, Schellenberg G, Tanzi R, Wasco W, Lannfelt L, Selkoe D, Younkin S. (1996). Secreted amyloid beta-protein similar to that in the senile plaques of Alzheimer's disease is increased in vivo by the presenilin 1 and 2 and APP mutations linked to familial Alzheimer's disease. *Nat Med* 2:864–870.
22. Schipper HM, Chertkow H, Mehindate K, Frankel D, Melmed C, Bergman H. (2000). Evaluation of heme oxygenase-1 as a systemic biological marker of sporadic AD. *Neurology* 54:1297–1304.
23. Stewart PA. (2000). Endothelial vesicles in the blood-brain barrier: are they related to permeability? *Cell Mol Neurobiol* 20:149–163.
24. Thomas T, Thomas G, McLendon C, Sutton T, Mullan M. (1996). Beta-amyloid-mediated vasoactivity and vascular endothelial damage. *Nature* 380:168–171.
25. Uyama O, Okamura N, Yanase M, Narita M, Kawabata K, Sugita M. (1988). Quantitative evaluation of vascular permeability in the gerbil brain after transient ischemia using Evans blue fluorescence. *J Cereb Blood Flow Metab* 8:282–284.
26. Vinters HV. (1987). Cerebral amyloid angiopathy. A critical review. *Stroke* 18:311–324.